ORIGINAL ARTICLE

ibausil
F. A. Finger-Institut für Baustoffkunde
Bauhaus-Universität Weimar

Activation of LC^3 binders by C-S-H nucleation seeding with a new tailored admixture for low-carbon cements

Ana Cuesta[1], Alejandro Morales-Cantero[1], Angeles G. De la Torre[1], Isabel Santacruz[1], Oliver Mazanec[2], Alessandro Dalla-Libera[3], Sebastien Dhers[2], Peter Schwesig[2], Pere Borralleras[4], and Miguel A.G. Aranda[1]

Correspondence

Dr. Ana Cuesta
Email: a_cuesta@uma.es
[1]Departamento de Química Inorgánica, Cristalografía y Mineralogía, Universidad de Málaga, Málaga 29071, Spain

[2]Master Builders Solutions Deutschland GmbH, Albert-Frank Str, 32, 83308 Trostberg, Germany

[3]Master Builders Solutions Italia Spa, Via Vicinale delle Corti, 21, 31100 Treviso, Italy

[4]Master Builders Solutions España S.L.U., Carretera de l´Hospitalet, 147-149, Edificio Viena, 1ª planta, 08940 Cornellà de Llobregat, Spain

Abstract

The use of supplementary cementitious materials is currently the most favorable strategy for reducing CO_2 emissions in cements. Limestone Calcined Clay Cements, LC^3, are a type of cement that allows the reduction of CO_2 emissions up to 40%. The proportions of the mixtures can vary, but the most investigated combination, LC^3-50, contains about 50 wt% clinker, 30 wt% calcined kaolinitic clay, 15 wt% limestone and an optimised calcium sulphate content. However, the mechanical strengths of LC^3 at early ages are not good enough and they should be improved. One way of doing this is by employing commercial strength-enhancing (accelerator) admixtures based on C-S-H nucleation seeding. For this work, LC^3-50 cements were prepared with clays with varying kaolinite contents. Mortars and pastes were fabricated using a new PCE-based superplasticizer developed to avoid the loss of fluidity at early ages typical of LC^3 binders. The selected accelerator for this study was Master X-Seed STE53. The results show that the loss of fluidity of LC^3 mortars during the first hours could be solved by a recently developed PCE-based superplasticizer. The compressive strengths at 1 day for LC^3 mortars strikingly improved by using the C-S-H seeding admixture and this behavior was maintained for up to 28 days.

Keywords

Calcined kaolinitic clay, admixtures, C-S-H nucleation seeding, superplasticizer, CO_2 footprint, mechanical strength

1 Introduction

Climate change is a fact and finding feasible strategies to reduce greenhouse gas emissions of industrial processes, while maintaining economic growth, is challenging but totally needed. Portland cement (PC) and concrete industries contribute to ~8% of the total anthropogenic CO_2 emissions [1], having into consideration the raw material decomposition (mainly calcite), and burning of fossil fuels in the kilns and milling processes. The use of supplementary cementitious materials (SCMs) [2,3], to reduce the Portland clinker factor, is currently the best strategy to reduce CO_2 emissions in the global cement industry [4]. The selection of these SCMs is key to maintaining the final performances of cement (for instance, mechanical performances and durability requirements).

Calcined clays are a type of SCMs that in combination with PC can contribute to reducing the CO_2 emissions [3]. The percentages of the mixtures can vary, but the most common combination is the LC^3-50 [5,6], which contains ~50 wt% of PC clinker, 30 wt% of calcined clay, 15 w% of limestone and an optimised amount of sulphate. This composition can lead to a reduction of around 40% in CO_2 emissions [7]. However, the two main drawbacks of the resulting binders are (1) their poor mechanical strengths at early ages [5] (i.e. 3 days or earlier); and (2) the loss of fluidity which is very important during the first 1-3 hours after mixing [8].

There are different possibilities to accelerate early age hydration reactions of LC^3 binders, one of them is the addition of chemical admixtures [9]. For instance, the addition of C-S-H seeding [10,11] or alkanolamines [12,13]. Furthermore, a synergistic effect between C-S-H seeding in combination with alkanolamines [14–16] is being very recently reported. This combination is a fast-growing field because it can be applied to low-carbon types of cement, for instance, to improve the mechanical strength and durability performances of LC^3 binders.

The work has aimed to boost the mechanical strength of LC^3 binders at early ages, using a commercial accelerator admixture based on C-S-H nucleation seeding, Master X-Seed STE53 (**STE53**), following our previous works for a plain PC [15,16]. Moreover, to improve the loss of fluidity, a new commercially available PCE-based superplasticizer has also been investigated, which was specially designed for tackling this issue.

2 Materials and Methods

2.1 Starting material

The following materials have been used for this work (i) CEM-I 52.5R, with $D_{v,50}$=12(1) μm, (ii) CC1, CC2 and CC3 that are three clays (calcined at 860 ºC with a $D_{v,50}$=13±2 μm) with variable kaolinite content, ~74, ~49 and ~29 wt%, respectively, (iii) limestone (from Omya Clariana S.L.U.) with a $D_{v,50}$~5 and (iv) gypsum (from yesos y escayolas La Maruxiña S.A.). The final binders, LC^3-50, were prepared with the following composition: 52 wt% of CEM-I 52.5R, 30 wt% of calcined clay, 15 wt% of limestone and 3 wt% of gypsum), (LC^3-CC#). PC-Ref refers to the plain PC. Finally, PC-Qz was prepared as a second reference sample by replacing just the calcined clay by (inert) quartz.

For the pastes/mortar preparations, two superplasticizers (SP-1 and SP-2) based on PCE and one admixture based on C-S-H nucleation seed with alkanolamines have been used. All of them are from Master Builders Solutions. SP-1 is a standard PCE-based SP used for concrete rheology optimisation. SP-2 is a new SP specially designed to avoid the loss of fluidity during the first hours of hydration in LC^3 based-systems. Master X-Seed STE53 (STE53) is C-S-H gel-based seeding admixture with a solid content close to 28 wt%.

2.2 Slump retention

Mortars have been prepared using a w/b (water-to-binder) mass ratio of 0.40 and with a s/b (sand-to-binder) mass ratio of 1.78 at a temperature of 20 ºC.

Firstly, the SP amount was optimised to have an initial constant mortar self-flow, i.e. 200±20 mm. Secondly, for the samples containing the STE53 admixture, a 2.00 wt% was added (by the weight of binder, referred as the commercial suspension).

The mortars were prepared using a mortar mixer (Matest, mod. E095) as follows: (i) 60 s at 140 rpm (solid, i.e. sand and binder and 80 wt% water); (ii) 30 s were needed to add the SP and 20 wt% of water for samples without C-S-H seeding or 10 wt% of water for samples with seeding; (iii) then, 60 s at 285 rpm; (iv) only for samples incorporating C-S-H seeding, 30 s to add the admixture and the 10 wt% of water left; (v) 120 s at 285 rpm. Finally, the mortar was poured into the truncated cone (bottom diameter: 100 mm, top diameter: 70 mm, height: 60 mm) in two steps. Firstly, half of the cone was filled up and a glass rod with 30 vertical punctures was used to take out the air bubbles. Secondly, the cone was filled up completely and punctured 30 times more. The flow measurements were performed at t_0, 30 and 60 min, at 20(2) ºC.

2.3 Isothermal calorimetry

For isothermal calorimetry, a Thermal Activity Monitor (TAM) instrument with eight channels was used. The pastes were prepared using a w/b mass ratio of 0.35 and with the same amount of SP optimised for the mortars. The pastes were prepared, using a mechanical stirrer (IKA, model RW20-D) following this protocol: (i) 60 s at 800 rpm (binder and 80 wt% water); (ii) 30 s by adding the SP and 20 wt% of water for samples without C-S-H seeding or 10 wt% of water for samples with seeding; (iii) 60 s at 800 rpm; (iv) this step is only for samples with C-S-H seeding, 30 s by adding the seeding and the 10 wt% of remain water and (v) 60 s at 800 rpm. The calorimetry measurements were performed for up to 7 days (without the first 45 minutes which were needed to reach thermal equilibrium) at 20 ºC.

2.4 Compressive strength

Mortars were prepared as described in section 2.2. The moulds of 4×4×16 cm were filled, kept and demoulded as previously reported [17]. The compressive strength measurements were performed following the EN196-1 using a press (Model Autotest 200/10 W, Ibertest) at a rate of 1.5 MPa·s^{-1}.

Three prisms per age were prepared and measured at 1, 7 and 28 days. The reported compressive values are the average of the six specimens, which resulted after flexural tests.

2.5 Mercury Intrusion Porosimetry (MIP)

For the MIP analysis, the binder pastes were prepared with the same protocol as that prepared for isothermal calorimetry. Then, they were inserted in Teflon moulds at 24 hours and kept in a saturated solution of portlandite up to the selected hydration age (1, 7, and 28 days). Before the measurements, the hydration was stopped with the following procedure: samples were immersed in isopropanol for 3 days and dried at 40 ºC. The porosity was measured by using a micromeritics AutoPore IV 9500 porosimeter (Micromeritics Instrument Corporation, Norcross, GA, USA) using the previously reported conditions [17].

2.6 Thermal Analysis (TA)

Thermal analyses were measured in arrested pastes (using the same protocol than that for LXRPD) using an SDT-Q600 analyser from TA instruments (New Castle, DE, USA). The data acquisition was performed from 40 ºC up to 1000 ºC. Before collecting data, the sample was maintained at 40 ºC for 30 min.

2.7 Laboratory X-Ray Powder Diffraction (LXRPD)

LXRPD measurements were collected with a D8 ADVANCE diffractometer (Bruker AXS) with a θ/θ configuration geometry using Mo–Kα_1 strictly monochromatic radiation (λ=0.7093 Å). The equipment is located at SCAI–Universidad de Málaga. The pastes were prepared as previously described. Before the measurements, the pastes were ground, washed and filtrated with isopropanol twice and once with diethyl ether. To collect the LXRPD data, the pastes were mixed with 20 wt% of α-Al_2O_3 (AlfaAesar), calcined at 1500 ºC during 12h and sieved <125 μm, as

internal standard. The ACn content (amorphous and crystalline non-determined) was calculated by using the internal standard protocol [18].
Finally, the powders were loaded between two Kapton foils before being measured. The quantitative analyses using the Rietveld methodology were performed with the GSAS suite of programs and the EXPGUI graphic interface [19].

3 Results and discussion

Firstly, the amounts of SP were optimised for each binder to have an initial constant self-flow of 200±20 mm. The flow values were measured at t_0 and also at 30 and 60 minutes to evaluate the slump retention, see Table 1. From the data reported in that table, we highlight the following observations: (i) The fluidity loss in LC^3 mortars with standard PCEs, i.e. SP-1, is very high for clays which contain high amounts of metakaolin (MK), i.e. CC1. This has been reported previously [20]; (ii) as it is already known, the amount of SP needed for LC^3 processing is a function of the MK content, which tends to correlate with BET surfaces. Consequently, the LC^3-CC1 mortar requires more SP-2 content, 1.2 wt%, than the LC^3-CC3 mortar, which only requires 0.5 wt%; and (iii) SP-2 successfully solved the slump retention problem, see Table 1. For example, for LC^3-CC1 with SP1 the fluidity drops in the first 30 min, however, it is maintained when SP2 is used.

Table 1 Optimised amounts of SPs, and slump values, at the given times, for the studied mortars.

Mortars	SP-1 (wt%)	SP-2 (wt%)	Slump /mm (t_0)	Slump /mm (30min)	Slump /mm (60min)
PC-Ref-a	0.34	-	183(1)	156(1)	143(2)
PC-Ref-b	-	1.20	190(1)	264(1)	288(1)
PC-Ref-c	-	0.80	156(1)	203(1)	231(4)
LC^3-CC1	1.00	-	196(2)	106(2)	100(1)
LC^3-CC1	-	1.20	186(3)	210(1)	196(1)
LC^3-CC2	-	1.00	214(2)	271(1)	284(1)
LC^3-CC3	-	0.50	210(1)	267(1)	276(3)
PC-Qz	-	0.40	211(1)	266(1)	283(1)

After addressing the slump retention problem, the second step was to improve the mechanical strengths of mortars at early ages by using an admixture, STE53, which contains C-S-H seeds. Initially, the effect of the C-S-H nucleation seeding admixture on the mechanical strengths of the mortars was studied, see Figure 1. Figure 1a displays the direct compressive strength values for the studied mortars at the selected ages of hydration. Figure 1b shows the same data but as percentages of the variation of the compressive strength values referred to PC-Ref at the same hydration times.

At 1 day of hydration, the mechanical strengths are lower for all the LC^3 binders in comparison with the PC-Ref. The 50 wt% of dilution due to the calcined clay and calcite would imply around 22 MPa at 1 day, but even smaller values were measured for some binders. As known, the reduction in the mechanical strength values is much lower at 7 and 28 days for these samples containing calcined kaolinitic clays. This reveals once more the drawback stated in the introduction, the low compressive strength values at very early ages. Finally, Figure 1 also shows a clear (and expected) trend: a lower amount of kaolinite/metakaolin implies lower mechanical strength values.

Chiefly, the addition of STE53 led to a large increase in the compressive strengths in all studied samples, see Figure 1. The seeded LC^3 binders with relatively low MK content, i.e. LC^3-CC2 and LC^3-CC3, developed more than 20 MPa at 1 day. C-S-H seeding improved the compressive strengths at 1 day of LC^3-CC1, -CC2 and –CC3, by 40%, 53% and 110% respectively. This astonishing result tackled the key drawback described in the introduction, meaning that clays with quite low kaolinite contents could be employed to prepare LC^3 binders with competitive performances. Moreover, at 7 days of hydration, the three seeded mortars showed an important increase in mechanical strength, in comparison with the unseeded ones. The relative improvements in the same order were 24%, 27% and 31%. The enhancement in the mechanical strengths was maintained at 28 days of hydration. The relative improvements were 29%, 25% and 33%. It is worth highlighting that at this hydration time, the LC^3 binder with the highest MK content, i.e. LC^3-CC1, has 88 MPa, 19 % relative increase concerning the plain PC, i.e. PC-Ref. This increase is very noteworthy keeping in mind that the binder has 50% less Portland cement.

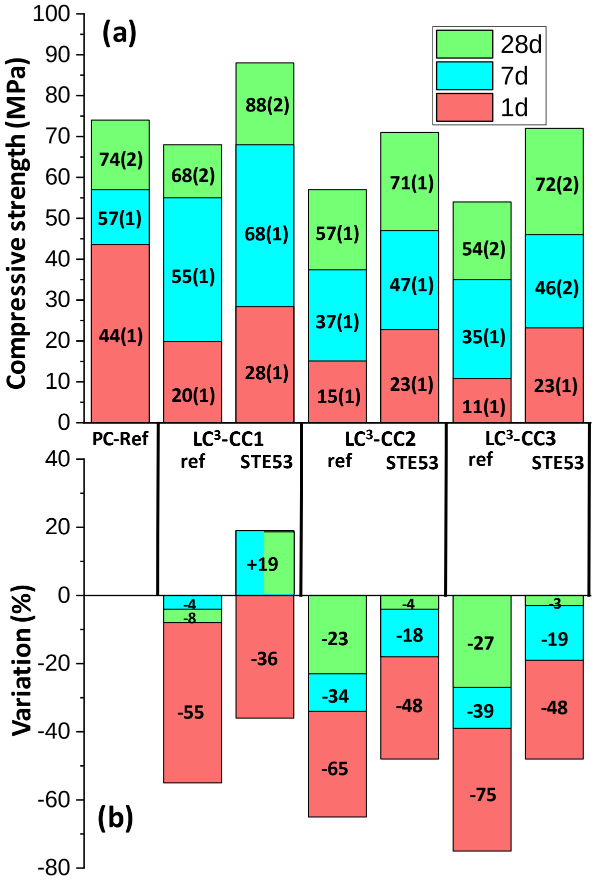

Figure 1 (a) Mortar compressive strengths for LC^3 samples without (ref) and with 2 wt% C-S-H seeding (STE53); (b) Variation of compressive strengths with respect to PC-Ref.

Additionally, the heat released by the corresponding pastes during the first 7 days was studied for samples with and without C-S-H seeding. Figure 2 shows the heat flow and cumulative heat curves. The top figures show the heat flows and the bottom ones the cumulative heat traces including the cumulative values at 1, 4 and 7 days of hydration. Firstly, we will discuss the results concerning the unseeded pastes: (i) LC^3 pastes released less heat compared to the PC-Ref sample, as expected. (ii) The total heat released by the sample containing quartz, PC-Qz, is lower than that of all LC^3 pastes, see the bottom left panel. (iii) Because the three LC^3 pastes released more heat at about 12 hours of hydration than the PC-Qz paste, used as a reference, this might indicate that the pozzolanic reactions are starting to develop around this time. (iv) Finally, it should be pointed out that the heat released by PC-Qz is higher than the expected value (i.e. 48% less heat due to dilution), which is very likely due to the filler effect as this quartz has a $D_{v,50}$ of 15 µm.

Secondly, we discuss the hydration acceleration effect observed for the seeded samples: (i) the induction periods are shortened in all the pastes with STE53, as shown in Figure 2 (top-right panel). This period ranged 1.3-2.8 h for the unseeded pastes and 1.0-1.8 h for the seeded ones. (ii) All the C-S-H seeded samples present higher slopes in the acceleration stages. (iii) At earlier ages, these pastes also display larger main peaks. This can be observed at 1 day of hydration, Figure 2, where all the curves show larger accumulated heat released at this time, see inset at the bottom. (iv) For the seeded pastes, the aluminate-related peaks are larger and sharper as can be observed in Figure 2 (top-right panel). Moreover, the aluminate peak is smaller in the PC-Qz sample, having the same amount of cement, consequently, it can be cautiously stated that the C-S-H seeding is also accelerating the aluminate dissolution from the calcined clays, i.e. MK. This is supported by the evidence that the height of the aluminate peak increases with the MK content as the surface does.

The pore size distributions and cumulative porosities for all the pastes are displayed in Figure 3. The MIP study was performed at 1, 7 and 28 days of hydration. It is important to point out that as mercury only intrudes the connected porosity at a given pressure, the MIP data show pore *entry* size distributions. Consequently, there is an underestimation of the volume of the biggest pores as only a fraction is accessible through the smaller ones, known as ink-bottle effect. In any case and with this caveat, MIP is widely used for the characterisation of the porosity features in binder materials. As expected, there is a decrease in the porosity with the hydration time. Moreover, the consequence in the microstructure due to the addition of the C-S-H nucleation seeding in the LC^3 binders deserve special attention.

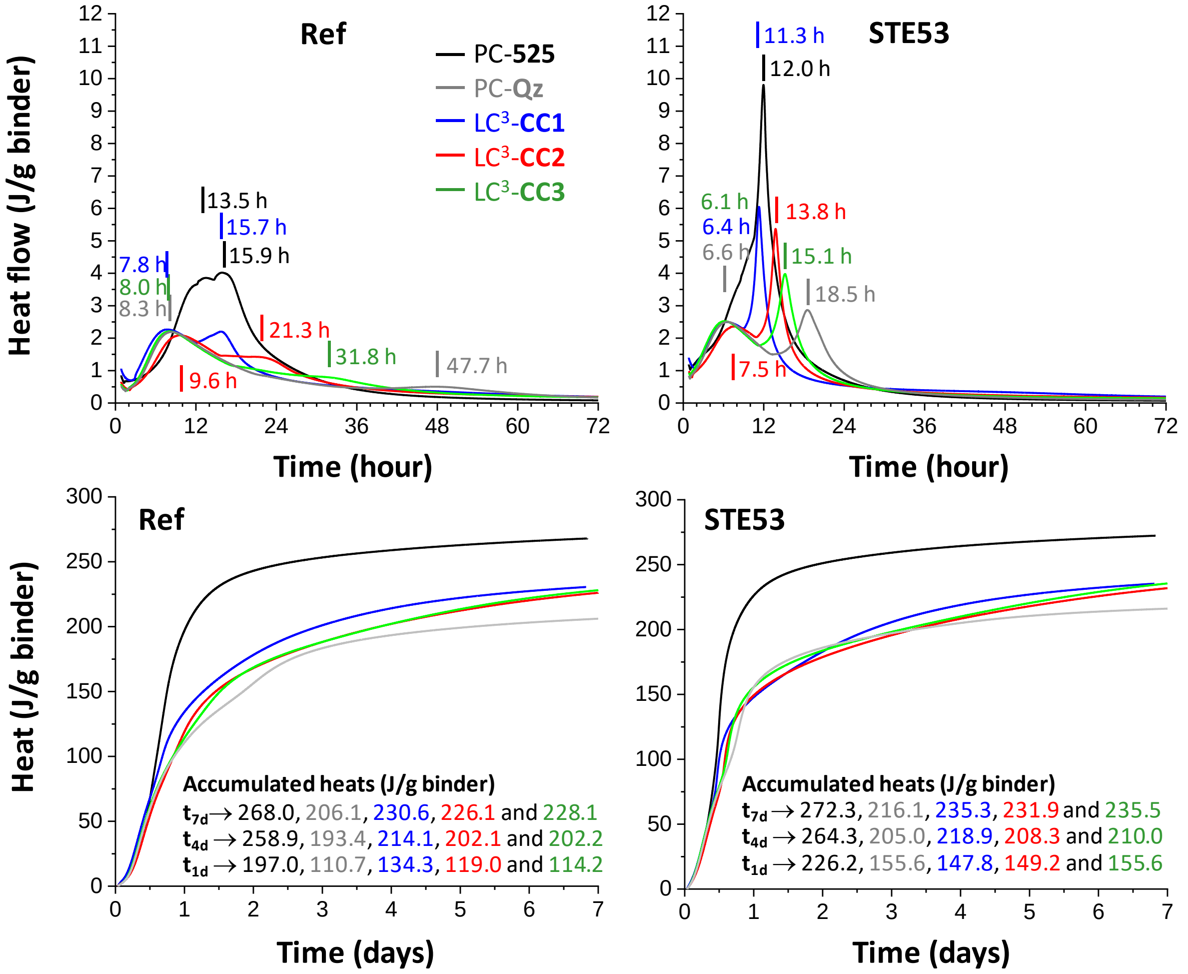

Figure 2 Calorimetric curves for pastes with w/b= 0.35. Heat flow (top) and total heat (bottom) released for pastes without seeding (left) and with seeding (right).

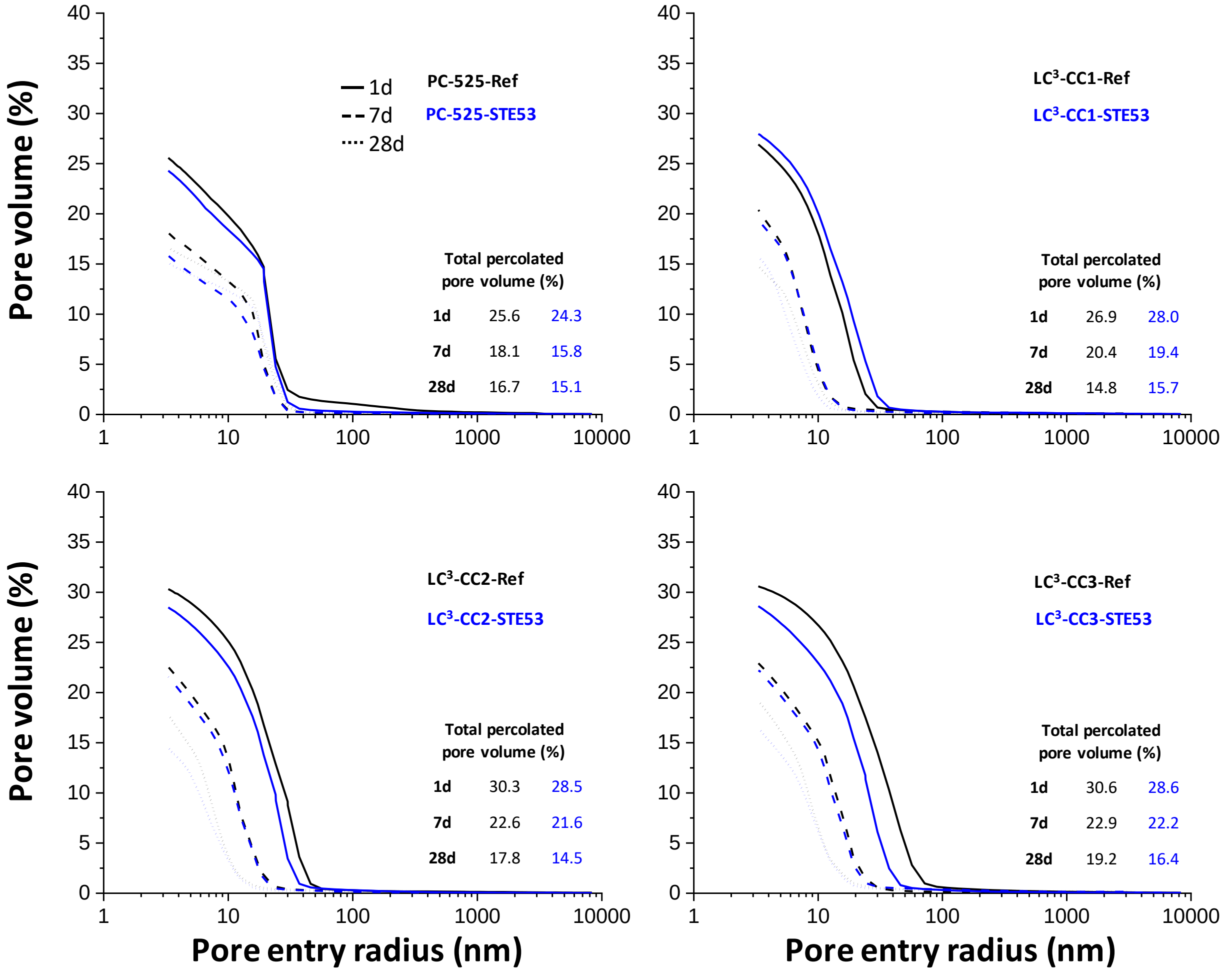

Figure 3 Cumulative porosity curves for all the studied binders at 1, 7 and 28 days of hydration.

Figure 3 shows that at 1 day of hydration, the pastes containing STE53 show a reduction of the threshold pore size in comparison with the unseeded ones. However, at 7 and 28 days of hydration, this improvement is not clearly shown as the threshold pore radii are much more similar for the seeded and unseeded pastes. Figure 3 also shows that, as expected, the total porosities are smaller for the seeded pastes at all the hydration ages in the PC-ref sample and in the LC^3 samples with CC2 and CC3. The LC^3-CC1 does not show this trend so clearly. Overall, it can be concluded that the addition of STE53 in the pastes reduces the total porosity and the threshold pore size. For the LC^3 pastes, the C-S-H seeding admixture seems to be more effective in decreasing the total porosities at 28 days of hydration.

Figure 4 shows the thermal traces for all the studied pastes (with and without seeding) at 1, 7, and 28 days of hydration. It can be observed that, for a given paste, the total weight losses increase with the hydration age, reflecting the progression of the hydration reactions. Moreover, for the seeded samples, the overall cement hydration activation by the admixture is deduced from a larger weight loss at all the hydration ages, which leads to a reduction of the free water (FW) content as it will be detailed in the LXRPD section. For instance, PC-525-Ref has a total weight loss of 14.5%, 19.9% and 21.1% at 1, 7 and 28 days of hydration, respectively. The corresponding losses for PC-525-STE53 are 18.7%, 21.8% and 22.8% at the same ages, respectively. This shows that the effect of the STE53 additive is stronger at early ages, as widely reported [10]. For the LC^3 pastes, the activation is more similar at all the hydration times. For instance, the total weight losses for the LC^3-CC1-Ref are 18.1%, 21.3% and 23.3% and those for LC^3-CC1-STE53 are 19.1%, 23.0% and 24.3% at 1, 7 and 28 days of hydration, respectively.

The portlandite contents are calculated using the tangential method [21] with the thermal analysis data, see Figure 4. The portlandite contents are calculated using the data that were collected for the arrested samples. For this reason, these data need to be referenced to the pastes containing the free water, neat pastes, in order to be comparable with the RQPA results. The correction factor (100-FW)/100 is applied to do this conversion.

Indeed, for the PC-525-Ref samples (unseeded and seeded), in the absence of pozzolanic reaction, the CH content increased with the hydration time, revealing the progression of the hydration reactions. For the LC^3 pastes, there is a reduction of the portlandite content with time, which demonstrates that the pozzolanic reaction is taking place. Moreover, PC-525-Ref shows 6.0 wt% of CH and LC^3-CC1-Ref 2.3 wt% at 1 day of hydration which proves that the pozzolanic reaction is already contributing at this age.

For the seeded samples, the CH content is slightly smaller than that for the corresponding unseeded samples at all the selected ages and in all the series. As it was previously reported [15,16], for the PC reference sample, this could be due to the smaller reactivity of the C_3S phase, a larger Ca/Si ratio of the resulting C-S-H gel, or because of the formation of the amorphous phases such as AFm-Hc which consume portlandite. Moreover, for the LC^3 series, the smaller CH contents could be a sign of enhanced pozzolanic reaction but the nuances listed above also apply. Hence, this is not further discussed here.

Finally, the LXRPD data, collected with an internal standard were acquired for all the pastes, with and without C-S-H nucleation seeding. The data were analysed by the Rietveld methodology. These analyses allow us to obtain the quantitative phase analysis including the ACn content. Tables 2-5 show these results including the FW values obtained by thermal analysis.

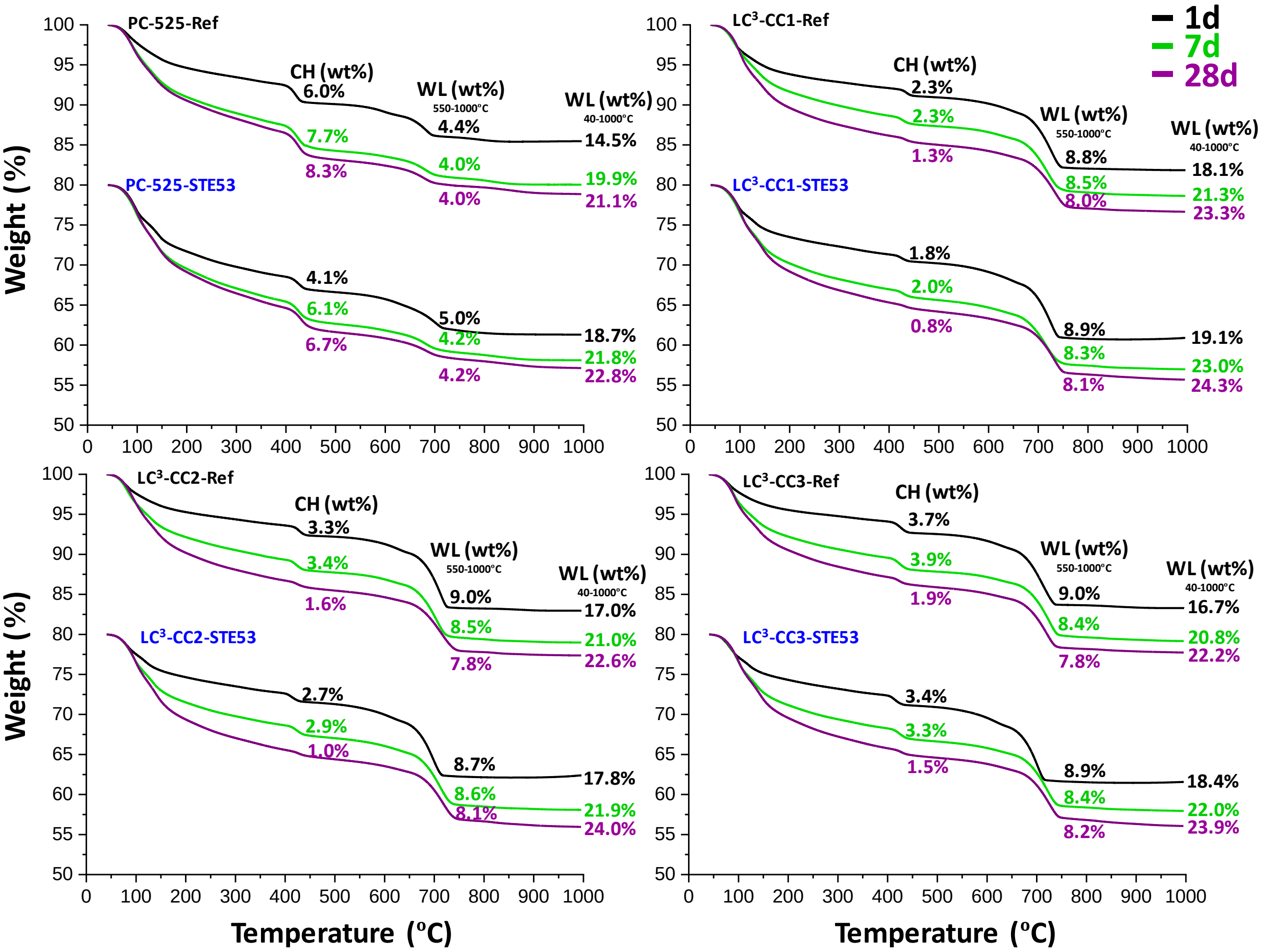

Figure 4 Thermal analysis traces for all the pastes after arresting the hydration and holding 30 min at 40 ºC. The curves for the different pastes have been vertically displaced for clarity. The portlandite, CH, contents (wt%) given refer to the neat pastes (containing the FW for easy comparison to the RQPA results). The total weight losses (WL) (wt%) are also showed.

Table 2 reports the data obtained for the PC-Ref paste and its corresponding seeded with STE53 analogue. Firstly, it is important to clarify that the w/c used here is 0.35, which was selected to have pastes with a similar consistency to that of the mortars. This value is low for a PC-52.5 cement for adequate hydration at later ages, i.e. smaller than ~0.42, and consequently, at 28 days of hydration there could not be enough water for the progress of the hydration reactions. The degree of reaction of alite at 28 days, 80-85%, is slightly lower than the commonly reported values at this hydration age, ~90%.

For the reference PC samples, it is observed that for the seeded paste there is a slight reduction in the reaction degree of the C_3S and consequently less CH is formed as it was also determined in the thermal analysis. Concerning the hydration degree of C_3A and C_4AF there is a clear acceleration and dissolution of these phases in the C-S-H seeded samples. The delay in the C_3S hydration reaction could be due to the enhancement of aluminate dissolution. Higher amounts of aluminate phases in the pore solution are known to delay C-S-H growth. The hydration degree of C_4AF is 36% at 1 day for the PC-525-Ref and 88% for the corresponding seeded paste, PC-525-STE53. For the C_3A, the hydration degree changes from 65% to 86 % at 1 day for PC-525-Ref and PC-525-STE53, respectively.

It is important to highlight that the overall hydration degree for the C-S-H seeded samples is invariably higher than that of the references. This is firmly established as the C-S-H seeded pastes always have smaller values for the FW contents.

Tables 3-5 show the RQPA results for the LC3 binders with and without C-S-H nucleation seeding. Several points can be discussed: (i) the amount of CH found at 1 day is lower than that expected from alite reactivity which indicates that the pozzolanic reaction is already taking place. Moreover, there is a clear reduction of the CH content from 7 to 28 days of hydration for all the LC^3 pastes, seeded and unseeded. These results agree with the thermal analysis observations. (ii) The amount of ettringite found in the pastes is lower than expected as a consequence of the arresting hydration protocol which severely damages AFt (and other sensitive phases). This could slightly alter the ACn contents. (iii) FW gives an idea of the reactivity of the pastes, as expected, this value decreased with time and is also lower in the C-S-H seeded pastes which again proves the increase in the reactivity of these pastes due to the activation effect of the admixture. Consequently, the LC^3 binders with the richest kaolinitic clay, CC1, show lower FW values at all ages of hydration. (iv) Again, as it was observed for the PC reference samples, in LC^3 binders the C_4AF reactivity in the seeded pastes is very high which proves that the hydration of this phase is activated by the combination of the C-S-H seeding and alkanolamines. For instance, the hydration degree of C_4AF is 41% at 1 day for LC^3-CC1-Ref and 67% for the corresponding seeded paste, LC^3-CC1-STE53. On the contrary, C_3S does not seem to be activated by the STE53 admixture in the selected experimental conditions. (v) It can be observed that STE53 increases the formation of AFm-Hc which is likely a sign of enhanced pozzolanic reaction.

Table 2 RQPA for PC-525-Ref and PC-525-STE53 pastes with a w/c mass ratio of 0.35 with ACn determined by the internal standard method and FW determined by TA. The degree of reaction (DoH) in % of the clinker phases are also included.

Phases	**PC-525**	**PC-525-Ref**			**PC-525-STE53**		
	t_0	**1d**	**7d**	**28d**	**1d**	**7d**	**28d**
C_3S	45.6	16.0	8.9	6.4	20.1	12.2	9.3
C_2S	6.8	5.8	6.3	6.3	5.9	5.9	6.0
C_4AF	8.9	5.7	2.8	2.1	1.1	0.8	0.5
C_3A	4.2	1.5	0.4	-	0.6	-	-
$C\bar{S}H_2$	0.8	0.4	0.3	-	0.4	-	-
$C\bar{S}H_{0.5}$	1.8	-	-	-	-	-	-
$C\bar{C}$	5.5	3.7	3.1	3.7	4.8	2.3	2.3
Qz	0.4	0.3	0.3	0.4	0.4	0.3	0.4
CH	-	6.8	8.8	8.5	4.7	7.4	7.9
AFt	-	3.2	5.7	5.4	6.0	6.8	6.1
AFm-Hc	-	-	0.3	-	0.9	1.6	1.0
AFm-Mc	-	-	-	0.7	-	-	2.3
ACn	-	39.0	51.2	55.8	40.9	51.7	55.3
FW	25.9	17.6	11.8	10.6	14.2	10.1	8.9
DoH C_3S	-	65	81	86	56	73	80
DoH C_2S	-	7	7	7	12	12	12
DoH C_4AF	-	36	69	76	88	91	94
DoH C_3A	-	65	91	100	86	100	100

Table 3 RQPA for LC^3-CC1-Ref and LC^3-CC1-STE53 pastes with a w/b mass ratio of 0.35 with ACn determined by the internal standard method and FW determined by TA. The degree of reaction (DoH) in % of the clinker phases are also included.

Phases	**LC^3-CC1**	**LC^3-CC1-Ref**			**LC^3-CC1-STE53**		
	t_0*	**1d**	**7d**	**28d**	**1d**	**7d**	**28d**
C_3S	23.7	6.8	2.0	1.1	7.6	1.5	0.9
C_2S	3.5	3.4	4.0	3.8	3.5	3.8	3.9
C_4AF	4.6	2.7	1.6	1.0	1.5	0.7	0.6
C_3A	2.2	0.3	-	-	-	-	-
$C\bar{S}H_2$	2.6	1.0	0.5	0.5	-	-	-
$C\bar{C}$	14.0	12.5	12.0	12.3	13.9	10.9	11.2
Minors	5.1	3.8	4.2	4.1	4.1	4.0	4.1
CH	-	2.6	2.8	1.6	1.8	1.8	0.7
AFt	-	2.9	5.8	6.6	6.1	6.3	6.1
AFm-Hc	-	-	0.5	0.4	0.6	1.9	1.4
ACn	17.4	45.5	51.5	56.0	43.4	56.0	59.6
FW	25.9	18.3	15.0	12.6	17.6	13.2	11.6
DoH C_3S	-	71	92	95	68	94	96
DoH C_2S	-	-	-	-	-	-	-
DoH C_4AF	-	41	65	78	67	85	87
DoH C_3A	-	86	100	100	100	100	100

*At t_0, this binder also contains 0.9 wt% of $C\bar{S}H_{0.5}$.

Table 4 RQPA for LC^3-CC2-Ref and LC^3-CC2-STE53 pastes with a w/b mass ratio of 0.35 with ACn determined by the internal standard method and FW determined by TA. The degree of reaction (DoH) in % of the clinker phases are also included.

Phases	**LC^3-CC2**	**LC^3-CC2-Ref**			**LC^3-CC2-STE53**		
	t_0*	**1d**	**7d**	**28d**	**1d**	**7d**	**28d**
C_3S	23.7	5.7	1.3	0.7	6.5	1.5	0.6
C_2S	3.5	3.5	4.2	4.2	3.1	3.3	3.8
C_4AF	4.6	3.5	2.0	1.1	1.5	1.1	-
C_3A	2.2	-	-	-	-	-	-
$C\bar{S}H_2$	2.6	0.4	-	-	-	-	-
$C\bar{C}$	14.0	12.9	11.3	11.9	12.8	10.9	11.2
Muscovite	8.1	7.9	8.3	8.3	8.4	8.4	8.4
Minors	2.7	2.5	2.1	2.2	2.2	2.3	2.4
CH	-	3.6	3.6	1.4	2.8	2.9	1.1
AFt	-	2.6	4.2	5.6	4.1	5.0	5.7
AFm-Hc	-	-	0.6	0.6	-	1.7	1.3
AFm-Mc	-	-	1.1	1.8	-	-	1.6
ACn	11.6	37.9	45.8	49.2	39.5	48.2	52.1
FW	25.9	19.4	15.3	13.0	18.5	14.6	11.9
DoH C_3S	-	76	95	97	73	94	97
DoH C_2S	-	-	-	-	-	-	-
DoH C_4AF	-	24	57	76	67	76	100
DoH C_3A	-	100	100	100	100	100	100

*At t_0, this binder also contains 0.9 wt% of $C\bar{S}H_{0.5}$.

Table 5 RQPA for LC^3-CC3-Ref and LC^3-CC3-STE53 pastes with a w/b mass ratio of 0.35 with ACn determined by the internal standard method and FW determined by TA. The degree of reaction (DoH) in % of the clinker phases are also included.

Phases	**LC^3-CC3**	**LC^3-CC3-Ref**			**LC^3-CC3-STE53**		
	t_0*	**1d**	**7d**	**28d**	**1d**	**7d**	**28d**
C_3S	23.7	4.9	1.0	0.6	5.8	1.0	0.6
C_2S	3.5	3.9	4.2	3.8	3.9	3.7	3.3
C_4AF	4.6	3.2	1.7	0.9	1.3	0.6	-
C_3A	2.2	0.6	-	-	-	-	-
$C\bar{S}H_2$	2.6	0.6	0.6	0.7	0.6	0.4	0.7
$C\bar{C}$	14.0	11.9	11.3	11.7	12.9	11.0	10.7
Qz	12.0	11.9	12.2	12.2	12.2	11.7	12.6
CH	-	3.8	3.9	1.7	3.0	3.7	1.4
AFt	-	3.4	4.8	6.5	4.2	6.1	6.3
AFm-Hc	-	-	0.4	0.3	0.5	1.6	1.3
ACn	10.4	36.2	44.3	48.0	37.6	46.1	50.8
FW	25.9	19.8	15.5	13.5	18.1	14.2	12.1
DoH C_3S	-	79	96	97	76	96	97
DoH C_2S	-	-	-	-	-	-	-
DoH C_4AF	-	30	63	80	72	87	100
DoH C_3A	-	73	100	100	100	100	100

*At t_0, this binder also contains 0.9 wt% of $C\bar{S}H_{0.5}$.

4 Conclusions

The following conclusions can be extracted from this work:

(i) The new PCE-based superplasticizer, SP2, specially designed to avoid the loss of fluidity during the first hours, is fully compatible with the studied LC^3 binders as it successfully addressed the slump retention drawback.

(ii) The C-S-H seeding studied here, STE53, improved the compressive strengths of seeded LC^3 binders at 1 day of hydration by 40-110% with respect to the non-seeded ones. The C-S-H seeded LC^3 mortars developed 23-28 MPa at 1 day, which proves that they are competitive for field applications. Moreover, compressive strength improvements are maintained at 7 and 28 days of hydration. For instance, the relative improvements at 28 days ranged 25-33%. This improvement is related to the reduction of the total porosity likely due to a more homogeneous C-S-H gel distribution in the binders.

(iii) The calorimetric study showed that the employed accelerator admixture not only accelerated the hydration of the clinker phases but the pozzolanic reaction(s) seems to be also enhanced.

(iv) STE53 admixture accelerated the hydration rates of calcium aluminate phases, C_3A and C_4AF, as deduced by the X-ray powder diffraction analyses.

(v) The thermal analysis studies corroborated the overall larger hydration of the C-S-H seed-containing binders, as there was a reduction in the FW content for all STE53-containing pastes.

Acknowledgements

Partial funding from PID2020-114650RB-I00 research grant, which is co-funded by ERDF, is gratefully acknowledged.

References

[1] Barcelo, L.; Kline, J.; Walenta, G.; Gartner, E. (2014) *Cement and carbon emissions*. Mater. Struct. 47,p. 1055–1065. https://doi.org/10.1617/s11527-013-0114-5.

[2] Juenger, M.C.G.; Siddique, R. (2015) *Recent advances in understanding the role of supplementary cementitious materials in concrete.* Cem. Concr. Res. *78*, p. 71–80. https://doi.org/10.1016/j.cemconres.2015.03.018.

[3] Juenger, M.C.G.; Snellings, R.; Bernal, S.A. (2019) *Supplementary cementitious materials: New sources, characterization, and performance insights.* Cem. Concr. Res. *122*,p. 257–273. https://doi.org/10.1016/J.CEMCONRES.2019.05.008.

[4] UN Environment; Scrivener, K.L.; John, V.M.; Gartner, E. (2018) *Eco-efficient cements: Potential, economically viable solutions for a low-CO2, cement-based materials industry.* Cem. Concr. Res. *114*, p. 2–26. https://doi.org/10.1016/j.cemconres.2018.03.015.

[5] Scrivener, K.L.; Martirena, F.; Bishnoi, S.; Maity, S. (2018) *Calcined clay limestone cements (LC3).* Cem. Concr. Res. *114*, p. 49–56. https://doi.org/10.1016/j.cemconres.2017.08.017.

[6] Zunino, F.; Scrivener, K.L. (2021) The reaction between metakaolin and limestone and its effect in porosity refinement and mechanical properties. *Cem. Concr. Res. 140*, 106307. https://doi.org/10.1016/j.cemconres.2020.106307.

[7] Sharma, M.; Bishnoi, S.; Martirena, F.; Scrivener, K. (2021) *Limestone calcined clay cement and concrete: A state-of-the-art review.* Cem. Concr. Res. *149*, 106564. https://doi.org/10.1016/j.cemconres.2021.106564.

[8] Akhlaghi, O.; Aytas, T.; Tatli, B.; Sezer, D.; Hodaei, A.; Favier, A.; Scrivener, K.L.; Menceloglu, Y.Z.; Akbulut, O. (2017) *Modified poly(carboxylate ether)-based superplasticizer for enhanced flowability of calcined clay-limestone-gypsum blended Portland cement.* Cem. Concr. Res. *101*, p. 114–122. https://doi.org/10.1016/j.cemconres.2017.08.028.

[9] Cheung, J.; Jeknavorian, A.; Roberts, L.; Silva, D. (2011) *Impact of admixtures on the hydration kinetics of Portland cement.* Cem. Concr. Res. *41*, p. 1289–1309. https://doi.org/10.1016/J.CEMCONRES.2011.03.005.

[10] Cuesta, A.; Morales, A.; De la Torre, A.G.; Aranda, M.A.G. (2023) *Recent advances in C-S-H nucleation seeding for improving cement performances.* Materials *16*, p. 1462. https://doi.org/https://doi.org/10.3390/ma16041462.

[11] John, E.; Matschei, T.; Stephan, D. (2018) *Nucleation seeding with calcium silicate hydrate – A review.* Cem. Concr. Res. *113*, p. 74–85. https://doi.org/10.1016/J.CEMCONRES.2018.07.003.

[12] Gartner, E.; Myers, D. (1993) *Influence of Tertiary Alkanolamines on Portland Cement Hydration.* J. Am. Ceram. Soc. *76*, p. 1521–1530. https://doi.org/10.1111/j.1151-2916.1993.tb03934.x.

[13] Zunino, F.; Scrivener, K.L. (2021) *Assessing the effect of alkanolamine grinding aids in limestone calcined clay cements hydration. Constr*. Build. Mater. *266*, p. 121293. https://doi.org/10.1016/j.conbuildmat.2020.121293.

[14] He, J.; Long, G.; Ma, K.; Xie, Y.; Cheng, Z. (2021) *Improvement of the Hydration of a Fly Ash-Cement System by the Synergic Action of Triethanolamine and C-S-H Seeding.* ACS Sustain. Chem. Eng. *9*, p. 2804–2815. https://doi.org/10.1021/acssuschemeng.0c08618.

[15] Morales-Cantero, A.; Cuesta, A.; De la Torre, A.G.; Mazanec, O.; Borralleras, P.; Weldert, K.S.; Gastaldi, D.; Canonico, F.; Aranda, M.A.G. (2022) *Portland and Belite Cement Hydration Acceleration by C-S-H Seeds with Variable w/c Ratios.* Materials *15*, p. 3553. https://doi.org/10.3390/MA15103553.

[16] Morales-Cantero, A.; Cuesta, A.; De la Torre, A.G.; Santacruz, I.; Mazanec, O.; Borralleras, P.; Weldert, K.S.; Gastaldi, D.; Canonico, F.; Aranda, M.A.G. (2022) *C-S-H seeding activation of Portland and Belite Cements: an enlightening in situ synchrotron powder diffraction study.* Cem. Concr. Res*. 161*, p. 106946. https://doi.org/10.1016/j.cemconres.2022.106946.

[17] Shirani, S.; Cuesta, A.; Morales-Cantero, A.; De la Torre, A.G.; Olbinado, M.P.; Aranda, M.A.G. (2021) *Influence of curing temperature on belite cement hydration: A comparative study with Portland cement.* Cem. Concr. Res. *147*, p. 106499. https://doi.org/10.1016/j.cemconres.2021.106499.

[18] De la Torre, A.G.; Bruque, S.; Aranda, M.A.G. (2001) *Rietveld quantitative amorphous content analysis. J*. Appl. Crystallogr. *34*, p. 196–202. https://doi.org/10.1107/S0021889801002485.

[19] Larson, A.C.; Von Dreele, R.B. (2004) *General structure analysis system (GSAS).* Los Alamos Natl. Lab. Rep. LAUR *748*, p. 86–748.

[20] Morales-Cantero, A.; De la Torre, A.G.; Cuesta, A.; Santacruz, I.; Mazanec, O.; Dalla-Libera, A.; Dhers, S.; Borralleras, P.; Aranda, M.A.G. *Activation of LC3 low-carbon cements by C-S-H seeding.* In Proceedings of the Proceedings of the 16th International Congress on the Chemistry of Cement, Bangkok, 2023. Submitted.

[21] Scrivener, K.L.; Snellings, R.; Lothenbach, B. (2016) *A Practical Guide to Microstructural Analysis of Cementitious Materials*. Florida, CRC Press: Boca Raton, ISBN 9781498738675.